Topological and chemical ordering induced by Ni and Nd in $Al_{87}Ni_7Nd_6$ metallic glass

Kyungsoo Ahn and Despina Louca
University of Virginia, Department of Physics, Charlottesville, Virginia 22904, USA

S. J. Poon
University of Virginia, Department of Physics, Charlottesville, Virginia 22904, USA

G. J. Shiflet
University of Virginia, Department of Materials Science and Engineering, Charlottesville, Virginia 22904, USA
(Received 3 October 2003; revised manuscript received 21 May 2004; published 7 December 2004)

The local atomic structure of $Al_{87}Ni_7Nd_6$ amorphous metallic glass was determined by neutron diffraction and the pair density function (PDF) analysis. The local environments of the transition metal and rare earth ions were separately determined using Ni (^{58}Ni and ^{60}Ni) and Nd (^{142}Nd and ^{144}Nd) isotopes with very different neutron scattering lengths to separate their contributions. A distinct pre-peak was observed in reciprocal space indicative of clustering, a feature commonly present in good glass forming systems. The intensity of the pre-peak changes significantly with the substitution of Ni isotope but not so with Nd, suggesting that the transition metal is a major component to this peak. Such clustering might be a manifestation of chemical short-range ordering that is enhanced with Ni. The local environments for the Ni and Nd ions determined by the isotope difference PDF analysis are fundamentally distinct because Ni and Nd interact differently with Al giving rise to unique topologies. In particular for Ni, Ni-Al bond lengths are anomalously short due to stronger Ni-Al interactions and the local environment consists of distinct pair correlations. In contrast, the local Nd environment is more disordered with two separate Nd-Al environments and possibly relatively weaker interactions.

DOI: 10.1103/PhysRevB.70.224103 PACS number(s): 61.12.−q, 71.55.Jv, 81.05.Kf, 61.43.Fs

I. INTRODUCTION

The synthesis of amorphous systems with a large glass forming ability has been a long standing issue in the field of metallic glasses. Only noble metal based amorphous alloys such as Pd-Ni-P and Pt-Ni-P were produced in the past in bulk amorphous form, until a new class of amorphous alloys, zirconium and lanthanide based systems, was discovered.[1] The reason for this is partly because glass formation is a very complex phenomenon that has defied rigorous scientific understanding. Inoue[2] had earlier suggested three general principles to guide the development of new bulk amorphous alloys. These are as follows: (1) a system must contain more than three elements; (2) the difference in the atomic size among the main constituent elements must be larger than 10%; and (3) the heat of mixing among the constituent elements must have large negative values. More recent advances in the field have contributed to a better understanding of the concepts and driving mechanisms possibly responsible for glass formation. These are the introduction of the concept of glass fragility by Angell,[3] the measurement of fragility for bulk glasses by Busch *et al.*,[4] and the development of the theory of atomic size factor in glass transition and glass formability by Egami and Waseda.[5]

It appears that the key to glass formation is to slow down the kinetics of crystallization in the supercooled liquid where two factors can contribute to such a slowing down: the first is low diffusivity in the supercooled liquid, and the second is a small heat of crystallization, or increase in the stability of the glass in the liquid state against crystallization. Many efforts have been made to synthesize new kinds of amorphous alloys following these empirical rules as guidelines particularly in the Zr and Al based systems[6–8] with some success. New amorphous alloys exhibiting a wide supercooled liquid region before crystallization, greater than 50 degrees, were found to form by melt spinning Zr-Al-M (M=Ni or Cu). These alloys consist of elements with a significant distribution of their atomic sizes. The largest thickness reported for the Zr system is claimed to be over 10 mm.[9] The first successful production of a homogeneously amorphous Al-based alloy was achieved in Al-(Fe or Co)- B ternary alloys,[10] followed by the production of Al-Fe-(Si or Ge) alloys.[11] However, these ternary amorphous alloys are extremely brittle and their tensile strength is as low as 50–150 MPa.

The discovery of a group of Al-TM-RE (TM= transition metal, RE= rare earth) metallic glasses with a remarkably high Al content (up to 90 at.%) were discovered independently by He, Poon and Shiflet, and Tsai, Inoue and Masumoto.[6,12] Previously studied compositions for the Al-TM-RE glass, where TM=iron, cobalt or nickel and RE =yttrium, gadolinium or cerium, include $Al_{87}Ni_5Y_8$, $Al_{90}Fe_5Ce_5$ and $Al_{87}Fe_{8.7}Gd_{4.3}$.[6,13] The amorphous phase is formed with an Al content as high as 84 at.% for samples prepared by the magnetron sputtering process and as high as 90 at.% for samples prepared by the melt spinning process. These materials are truly noncrystalline alloys and combine the properties of a metal with the short range order of a glass. They are very homogeneous and lack defects such as grain boundaries and dislocations, typical of crystalline materials. The homogeneity and lack of grain boundaries have led to a number of remarkable mechanical and magnetic properties.[14]

Neutron and x-ray structural studies of melt spun $Al_{90}Fe_xCe_{10-x}$ alloys revealed strong interactions in the vicinity of the first coordination sphere for Fe.[15] The Fe-Al bond lengths were found to be short with a suggested 8% contraction, and a low coordination number with a 45% reduction from values based on dense-random-packing (DRP) of a hard spheres model. However Ce-Al bonds showed relatively smaller changes with a 5% reduction in the bond length and a 13% reduction in the coordination number from the expected values based on the DRP model. These anomalous effects observed for the Fe-Al bonds in the amorphous phase indicate a strong interaction between the Fe and Al atoms that may be in response to the increase in the covalency between the ions and a reduction in their metallic character.

In this paper, the atomic structure of the $Al_{87}Ni_7Nd_6$ amorphous alloy using pulsed neutron diffraction is reported. By using isotopes for Ni and Nd, ^{58}Ni, ^{60}Ni, ^{142}Nd and ^{144}Nd, the local environments for the transition metal and the rare earth ion were differentiated. From the atom specific structure function, a pre-peak at 1.5 $Å^{-1}$ is identified that changes intensity primarily with Ni isotopic substitution but very little with Nd substitution. This is indicative for the presence of chemical short range ordering (CSRO) that is enhanced by the transition metal in this system. The CSRO has been observed in other glass systems and is consistent with good glass forming ability. The local atomic structure determined by the isotope difference pair density function (DPDF) technique showed that the short range environment of Ni is significantly different from that of Nd giving rise to a different topological order for each element. The differences between the two environments are not merely attributed to differences in their atomic size but to their different interactions with Al. In the case of Ni, the DPDF function corresponding to the local structure consists of sharp features with well defined peaks. The Ni-Al coordination consists of ~11 nearest neighbors which compares to the coordination number calculated from a DRP model. This is markedly different from the AlFeCe system where a reduced coordination number was observed. At the same time, the Ni-Al bond length (2.46 Å) is shorter than expected assuming a metallic character of the bond similarly to what was observed for the Fe-Al bond in the AlFeCe alloy. On the other hand, Nd's bonding to Al shows no contraction while two different local Nd-Al environments are observed. The majority of Nd-Al pairs are essentially described assuming metallic bonding while a small number of Nd-Al pairs have slightly larger bonds. In addition, the Nd-Al coordination is actually enhanced, ~14 pairs for the first pair and ~4 for the second pair, not too far off the value of 16.4 calculated from a DRP model. The local environment of Nd in the ternary glass is comparable to the one found in the $Al_{88}Nd_{12}$ binary glass. This suggests that Nd is the glass forming element that destroys the Al crystallinity by the size effect, but its accommodation in the structure is nonspecific. On the other hand, the addition of Ni improves the strength of the ternary glass and its forming ability.

II. SAMPLE PREPARATION AND DATA ANALYSIS

A. Sample preparation

Five alloy ingots were prepared by melting nominal amounts of high-purity elements in an arc furnace under a partial argon atmosphere. The ingots were flipped over after each melting to improve homogeneity. The total weight loss after melting for 4 times was less than 0.6 wt%. One alloy was made from naturally abundant Ni and Nd elements, and four alloys were prepared using isotopes purchased from Oak Ridge National Laboratory. The isotopes were ^{58}Ni (99.93 at.%), ^{60}Ni (99.69 at.%), ^{142}Nd (97.86 at.%) and ^{144}Nd (97.30 at.%) in metal form. Amorphous ribbons of $Al_{87}Ni_7Nd_6$ were prepared from the pre-alloyed ingot by the single wheel melt-spinning technique under a partial helium atmosphere using a copper wheel (20 cm in diameter) with a typical circumferential velocity of 40 m/s. Typical dimensions were 15 mm thick, 1–2 mm wide and up to several meters long. The amorphous nature of the quenched ribbons was verified by x-ray diffraction and transmission electron microscopy. The melt spun ribbons were very flexible and could easily be bent in half without fracturing. All samples were prepared in identical conditions. The isotope alloys consisted of $Al_{87}{}^{58}Ni_7Nd_6$, $Al_{87}{}^{60}Ni_7Nd_6$, $Al_{87}Ni_7{}^{142}Nd_6$ and $Al_{87}Ni_7{}^{144}Ni_6$.

B. Neutron diffraction experiment and data analysis

The experiments were performed at the Intense Pulsed Neutron Source (IPNS) of the Argonne National Laboratory using the Special Environment Power Diffractometer (SEPD) and data were collected at room temperature for a total of 20 hours per sample in vacuum. About 3 grams of the sample in a ribbon shape was used in each experiment and loaded in a thin-walled vanadium can. The diffraction data were corrected for the instrumental background, and vanadium container scattering, and were normalized by the spectrum flux obtained from measuring a vanadium rod. In addition, standard absorption, inelasticity and multiple scattering corrections were applied. The structure function, $S(Q)$, determined from the diffraction data of the 4 isotope alloys, was normalized by the neutron scattering lengths for ^{58}Ni(b =14.4 fm), ^{60}Ni(b=2.8 fm), ^{142}Nd(b=7.7 fm) and ^{144}Nd(b =2.8 fm).[16] The total structure factor for one element α with one isotope 1 can be written using the following expression:

$$S_1(Q) = \frac{1}{\langle b_1\rangle^2}\left[(c_\alpha b_{\alpha 1})^2 S_{\alpha\alpha}(Q) + 2c_\alpha b_{\alpha 1}\sum_{\beta\neq\alpha} c_\beta b_\beta S_{\alpha\beta}(Q) + \sum_{\beta\gamma\neq\alpha} c_\beta b_\beta c_\gamma b_\gamma S_{\beta\gamma}(Q)\right], \quad (1)$$

$$\langle b_1\rangle = c_\alpha b_{\alpha 1} + \sum_{\beta\neq\alpha} c_\beta b_\beta, \quad (2)$$

where Q is the momentum transfer ($4\pi \sin\theta/\lambda$), c_α is the atomic fraction, and b_α is the neutron scattering length of element α with isotope 1.[17] Data were collected up to 33 $Å^{-1}$.

TABLE I. A list of $\langle b\rangle^2$ values used in the normalization of the $S(Q)$ and PDF.

Alloy	$\langle b\rangle^2$
$Al_{87}Ni_7Nd_6$-natural	0.1750
$Al_{87}{}^{58}Ni_7Nd_6$	0.1998
$Al_{87}{}^{60}Ni_7Nd_6$	0.1338
$Al_{87}Ni_7{}^{144}Nd_6$	0.1750
$Al_{87}Ni_7{}^{144}Nd_6$	0.1513

The pair density function (PDF), $\rho(r)$, is a real space representation of atomic correlations obtained through a Fourier transformation of the $S(Q)$:[18]

$$\rho(r) = \rho_0 + \frac{1}{2\pi^2 r}\int_0^{Q_{\max}} Q[S(Q)-1]\sin(Qr)dQ, \qquad (3)$$

where ρ_0 is the average atomic number density of the sample. The value of ρ_0 used in the analysis was $\sim$0.08. The PDF function represents the probability of finding pairs of atoms at a given distance.[19] Theoretically the Fourier integration should be carried out to $Q=\infty$, but in reality it is terminated to a finite value of Q determined by the wavelength of the probe. The PDF's of the isotope samples were processed under identical conditions using the same termination $Q_{\max}$ as well as the same background subtraction. The highest $Q_{\max}$ used in the analysis was 27 Å^{-1}. The subtraction of $\rho(r)$ of one isotope material from the other at a constant temperature provides the difference PDF (DPDF) with respect to Ni or Nd.[20] It is normalized by the corresponding average scattering lengths, $\langle b_1\rangle^2$, so that the true intensity is recovered and the difference in the peak amplitude is only due to the difference in the neutron scattering amplitude of Ni or Nd:

$$\mathrm{DPDF} = [\langle b_{^{58}\mathrm{Ni}}\rangle^2\rho(r)_{^{58}\mathrm{Ni}} - \langle b_{^{60}\mathrm{Ni}}\rangle^2\rho(r)_{^{60}\mathrm{Ni}}]. \qquad (4)$$

The values of $\langle b_1\rangle^2$ are listed in Table I. A similar expression can be written for Nd as well. Any pair that does not include Ni (or Nd) will be subtracted out because their scattering lengths do not change. The resulting DPDF provides the local atomic structure with respect to Ni (or Nd). This allows us to distinguish the contributions to the peaks from specific elements. The subtraction is done both in real and in reciprocal space and the results are identical.[20]

The area under the PDF peaks corresponds to the coordination number between pairs of atoms at specific interatomic distances. The number of β atoms around an α atom is given by the radial distribution function (RDF) $(4\pi r^2\rho(r))$ using the following expression:

$$N_{\alpha\beta} = \int_{r_{\min}}^{r_{\max}} 4\pi r^2\rho(r)dr. \qquad (5)$$

If a peak is composed of α and β bonds only, $N_{\alpha\beta}$ can be determined by integrating $4\pi r^2\rho(r)$ over the region, incorporating the peak in question and multiplying it by $\langle b\rangle^2/c_\alpha b_\alpha b_\beta$.

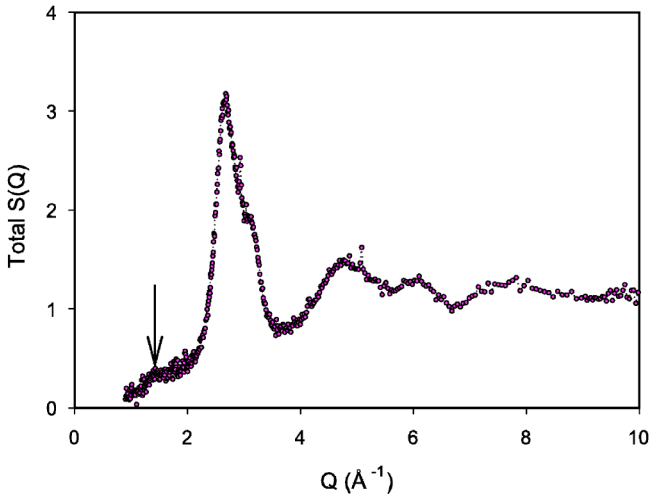

FIG. 1. The total structure function for natural $Al_{87}Ni_7Nd_6$.

III. RESULTS

A. Chemical clustering

The $S(Q)$ determined from the diffraction data for all five samples are shown in Figs. 1–3. In Fig. 1, the $S(Q)$ for $Al_{87}Ni_7Nd_6$ without isotope substitution shows a small pre-peak at $\sim$1.5 Å^{-1} in addition to the main features. The pre-peak has been observed in other metallic glass systems as well as in covalent glasses.[15,21] Separate studies on Fe based glasses have shown that the appearance of the pre-peak corresponds to good glass forming ability and an increase of the bulk glass size.[22] For example, in the ternary $Fe_{68}Zr_{10}B_{22}$ glass, the pre-peak is absent from the $S(Q)$, but when Mn is added to the system the pre-peak emerges. With Mn, the bulk glass formability improves and alloys can be prepared as large ingots several millimeters in diameter.[23] The pre-peak arises from correlations in the medium range structure and

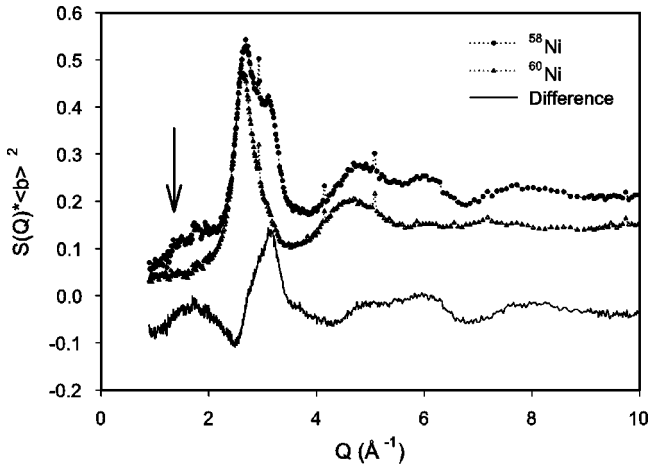

FIG. 2. The structure function determined for $Al_{87}{}^{58}Ni_7Nd_6$ is compared to the $S(Q)$ for $Al_{87}{}^{60}Ni_7Nd_6$. Also plotted in this figure is the difference between the two isotopes. Note how the intensity around the pre-peak region changes significantly with the ^{58}Ni isotope in comparison to the $S(Q)$ for the natural sample. Data are only plotted up to 10 Å^{-1} for clarity.

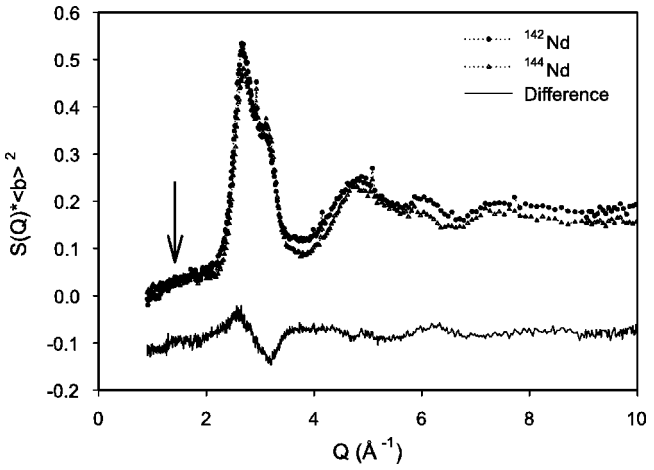

FIG. 3. The structure function determined for $Al_{87}Ni_7{}^{142}Nd_6$ is compared to the $S(Q)$ for $Al_{87}Ni_7{}^{144}Nd_6$. The difference between the two isotopes shows a very small change in the intensity of the pre-peak. Note how the intensity does not change much with the Nd isotopic substitution.

serves as a signature for ordering. To determine the chemical origin of this pre-peak, the Al glass was prepared using two isotopes of Ni and Nd. The properties of the glass do not change with the substitution. When Ni and Nd isotopes are used, the differences observed in the $S(Q)$'s shown in Figs. 2 and 3 are due to the difference in the scattering lengths of the isotopes. When the $S(Q)$ of ^{58}Ni is compared to the $S(Q)$ determined for the glass using ^{60}Ni, the intensity of the pre-peak decreases. The intensity changes because the neutron scattering lengths for the two elements are substantially different. ^{58}Ni is a quite strong neutron scatterer and is over five times stronger than ^{60}Ni. The difference between the two structure functions also shown in the figure (lower plot) isolates the contribution of Ni and makes it clear that the intensity around the pre-peak region is affected with this isotopic substitution. This indicates that Ni contributes significantly to the pre-peak region of the $S(Q)$.

With Nd isotopic substitution, very little change in the intensity of the pre-peak is observed (Fig. 3). The difference plot (the lower plot in Fig. 3) shows a slight modulation of the intensity around the pre-peak region. Although the scattering of the ^{142}Nd isotope is $2\frac{3}{4}$ times larger than ^{144}Nd and it is not as strong of a neutron scatterer as Ni, Nd contributes significantly less to the pre-peak than does Ni. Thus the presence of the pre-peak might suggest the existence of clusters with Ni as the center atom. The coherence length of the concentration fluctuations was estimated to be about 18 Å, obtained by fitting a Gaussian function to the pre-peak. From the position of the pre-peak it is possible to determine the real-space modulation of such chemical short-range ordering from $R(\text{Å}) \sim 7.5/Q(\text{Å}^{-1})$, where $R(\text{Å})$ is the correlation length between clusters.[24] This corresponds to about 5 Å.

B. Local atomic structure

The total PDF determined from the neutron data collected for natural $Al_{87}Ni_7Nd_6$ is shown in Fig. 4(a). Since the total PDF is a superposition of all pairs of atoms, it is difficult to resolve individual contributions from different elements. The first nearest neighbor peak in the total PDF consists of at least three different pair correlations, Al–Al, Al–Ni and Al–Nd. The overlap of the three pairs with somewhat different bonds contributes to the peak width. Subsequent peaks are even broader because of the overlap of several bonds with very similar lengths, and becomes more difficult to resolve between pairs. With the isotope substitution, the intensity is scaled by the scattering length as shown in Eq. (1), and the DPDF is the difference of the scattering intensity between two isotopes of the same element [Eq. (4)], eliminating contributions from elements whose b remains unchanged. Figure 4(b) and 4(c) are plots of the DPDF's for Ni and Nd, respectively. The DPDF's consist of pair correlations that involve either Ni or Nd only, thus their local environments are resolved in a way analogous to the XAFS technique although the plots in Figs. 4(b) and 4(c) are not partial functions.

1. Ni local environment

The first peak in the Ni-DPDF [Fig. 4(b)] at 2.46 Å is quite sharp with FWHM $\simeq$ 0.7, and corresponds to the first nearest Ni-Al pairs. The sharpness of this peak indicates that the Ni-Al bonds are about the same length in the entire space. The second small peak at 3.4 Å corresponds to the second nearest Ni-Al pairs. Subsequent peaks correspond to Ni-Nd at $\sim$5 Å and higher order Al-Ni and Ni-Ni correlations. Note that if metallic radii are assumed for Ni-Nd, a peak should appear at $\sim$3.06 Å but no such peak is observed, suggesting that Ni and Nd ions are most likely repelling each other. This could be a relevant factor to glass formation where the solute ion repulsions might invoke different interactions with the solvent. The first peak of the Ni-Al pair is actually shorter than the expected sum of the atomic radii for Al (1.43 Å) and Ni (1.24 Å) assuming metallic bonding (2.67 Å) by about 0.2 Å, an 8% contraction. A similar effect was previously observed in the Al-Fe-Ce system.[15] The shortening of the Ni-Al bond indicates strong Ni-Al interactions. From the electronic structure point of view, it is possible that electrons with an *sp* character of the Al atoms are transferred to the *d* states of the Ni atoms. Thus Ni enhances interactions with Al as seen by the shortening of Ni-Al bonds while topological short range ordering is invoked.

2. Nd local environment

The Nd-DPDF of Fig. 4(c) appears noisier because the difference in the scattering intensity between the Nd isotopes is smaller than for Ni but the main features are clearly distinguishable. The oscillations in the region prior to the first peak at around 3.3 Å are due to small differences in the total PDF's for the two Nd isotope samples. This is because each sample contains different amounts of small regions of crystalline Al. The first main peak is split to two corresponding to two Nd-Al bonds. The region under the peaks was fit by two Gaussians to separate their coordination as well as their bond lengths. This yielded one Nd-Al bond centered at

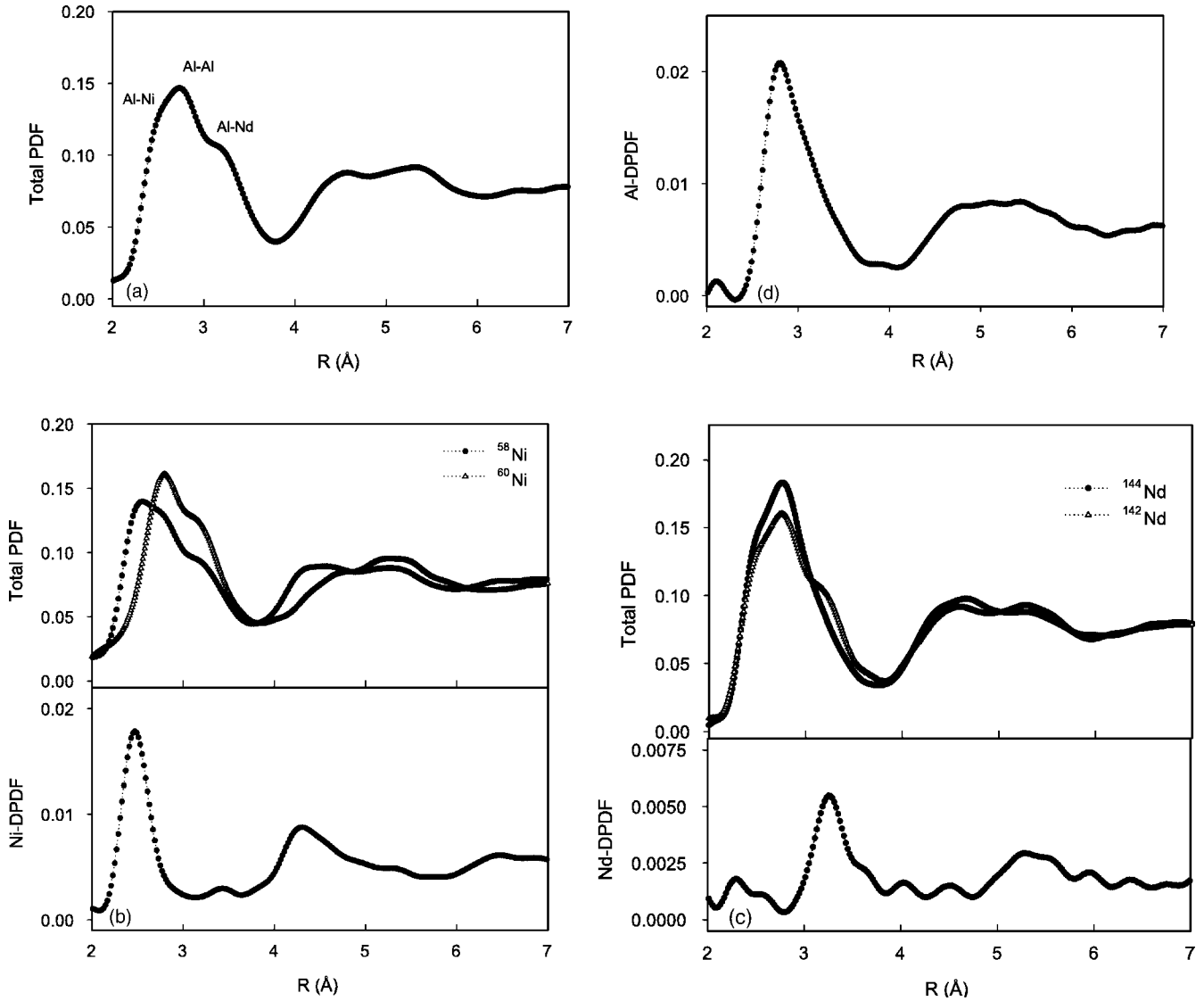

FIG. 4. (a) A plot of the total PDF for natural $Al_{87}Ni_7Nd_6$. (b) A plot of the PDF for $Al_{87}{}^{58}Ni_7Nd_6$ and $Al_{87}{}^{60}Ni_7Nd_6$. Also shown in this figure is the Ni-DPDF. (c) A plot of the PDF for $Al_{87}Ni_7{}^{142}Nd_6$, $Al_{87}Ni_7{}^{144}Nd_6$ and the Nd-DPDF. The DPDF of Nd is more noisy than that for Ni because of the smaller difference in the scattering length between the two isotopes. (d) By subtracting the Ni- and Nd-DPDF's from the total PDF, the Al-"DPDF" is obtained that consists primarily of Al correlations.

3.26 Å and another at 3.61 Å. Note that no Ni-Nd peak is observed in this DPDF either, further supporting the notion that Ni-Nd ions repel each other. The Nd-Al bond length at 3.26 Å is actually close to the expected value assuming metallic bonding with no contraction. In addition, since no chemical short-range ordering is promoted by Nd (no contribution to the pre-peak) it might indicate that Nd is distributed randomly. The local structure of Nd is quite similar to the one determined for binary glass $Al_{88}Nd_{12}$ (not shown). This suggests that because of its size, Nd becomes the glass forming element by destroying the Al crystallinity. On the other hand, the glass strength appears to be increasing by Ni alloying.

3. Al "local" environment

By subtracting the DPDF's determined for Ni and Nd from the total PDF, a function is obtained that mostly consists of Al correlations [Fig. 4(d)]. This function is not an Al-DPDF as in the other two cases, because it is not obtained by considering the difference between two Al isotopes (Al has only one isotope). Thus, in the Al-"DPDF," a small contribution from Ni and Nd pairs remains after the subtraction because the Ni and Nd DPDF's contain the difference of the scattering length between the two isotopes of Ni and Nd and not the actual values as in the total function. However, because of the high concentration of Al, the Ni and Nd contributions are minimal. From this figure it can be seen that the first peak corresponding to Al-Al correlations is quite broad. Although the average metallic bond for Al-Al is 2.86 Å, from the local atomic structure represented in this figure it can be seen that three peaks are present in this glass, at 2.69, 2.82 and 3.10 Å obtained from fitting the peak by three Gaussian functions. This suggests that the local structure of Al is modified in the presence of the TM and the RE.

TABLE II. A list of the peak positions (bond length) and coordination numbers (CN) for the $Al_{87}Ni_7Nd_6$ determined from the Ni- and Nd-DPDF's and also estimated from the DRP model. Also listed are the estimated bond lengths based on the sum of the metallic radii for the elements. The limits of integration used for calculating the coordination numbers are given. For the Nd ion, two Gaussian functions were fit within the given range to extract the coordination for the two peaks.

Pair	Bond length (Å)		CN		Limits in $N_{\alpha\beta}$	
	Expt	Est	DPDF	DRP	r_{min}	r_{max}
Al-Ni(1)	2.46±0.02	2.678	11.1±0.6	10.9	2.10	2.90
Al-Ni(2)	3.43±0.02		3.0±0.2		3.15	3.65
Al-Nd(1)	3.26±0.02	3.246	13.7±0.4	16.4	2.80	3.85
Al-Nd(2)	3.60±0.02		4.0±0.8			

4. Local coordination

To quantify the number of pairs contributing to the local environments around Ni and Nd, the coordination numbers (CN) are estimated from Eq. (5). These are listed in Table II. The Al coordination around Ni atoms calculated from the area under the peak is about 11 for the first peak and 3.0 for the second peak. The CN of the first nearest neighbor Al to Nd is 13.7 and the CN of the next nearest neighbor is determined to be 4.0. These numbers can be directly compared to the values estimated with the DRP model.[25] Using a binary glass as a model, Egami *et al.*[26] estimated the coordination based on the size ratios between two species of atoms. Such a model predicts the Al coordination number around Ni atom to be 10.9, which is close to the coordination number found experimentally for this system. For Nd, the calculated value is estimated to be 16.4 which is not too far from the value found experimentally.

IV. DISCUSSION

The results reported in this paper suggest a significant departure from a homogeneous atomic arrangement. The DPDF analysis shows that Ni and Nd atoms have very different local environments. Local Ni-Al clustering exists and the shortening of the Al-Ni distance indicates strong interactions between the two elements. On the other hand, the local Nd environment is more disordered with two distinct distributions of Al-Nd pair correlations and weaker clustering. The combined local environments of Ni and Nd can form the basic building block for constructing the entire structure. There are indications however that the Al sublattice is not so simple, as indicated by the "DPDF" for Al which would make it physically difficult to fill the entire space by simply considering the Ni and Nd environments. For this reason, it would be necessary to consider the changes of the electronic structure of Al in detail.[27]

The transition metal and the rare-earth ions have very different local environments. In the case of Ni, the sharpness of the DPDF features suggests that it forms a quasi-periodic lattice with distinct pair correlations in space. Also, the existence of the pre-peak in reciprocal space supports the presence of compositional and geometrical order around Ni. The sharpness of the first nearest neighbor Ni-Al peak indicates that Al atoms surround the Ni uniformly. In contrast, the Nd sublattice is not as well defined. Because of the larger size of Nd compared to Ni, Nd atoms are coordinated with more Al atoms than Ni. Evidence for Nd geometrical ordering is relatively weak and the broadening of the DPDF local structure peaks suggests that the arrangement of Al around Nd is less specific.

Evidence for Ni-Nd direct bonds has also not been observed and this suggests that interactions between these two atoms are repulsive. They are connected indirectly through Al atoms, supported by the existence of a second nearest Al neighbor to Nd at 3.61 Å and a second nearest Al neighbor to Ni at 3.4 Å. Therefore interactions between Ni and Nd atoms are through second nearest Al neighbors. In conclusion, the local atomic structure of the $Al_{87}Ni_7Nd_6$ amorphous alloy was investigated by pulsed neutron diffraction and the isotope difference pair density function analysis method. Both chemical and topological ordering are inferred from these findings that are primarily attributed to be due to Ni. Ni is what makes this glass strong.

ACKNOWLEDGMENTS

The authors would like to acknowledge valuable discussions with T. Egami, M. Widom, D. Nicholson, and Y. Wang. They also thank S. Short and J. Jorgensen for their assistance with the SEPD experiment. The work was performed under the auspices of the Boeing Company under Contract No. P.O.Z10687 at the University of Virginia. The IPNS of Argonne National Laboratory is supported by the U.S. Department of Energy under Contract No. W-31-109-Eng-38.

[1] A. Inoue, T. Zhang, and T. Masumoto, Mater. Trans., JIM **31**, 177 (1990).
[2] A. Inoue, Mater. Trans., JIM **36**, 866 (1995).
[3] C. A. Angell, Science **267**, 1924 (1995).
[4] R. Busch, A. Mauhr, E. Bakke, and W. L. Johnson, Mater. Sci. Forum **269–272**, 547 (1998).
[5] T. Egami and Y. Waseda, J. Non-Cryst. Solids **64**, 113 (1984).
[6] Y. He, S. J. Poon, and G. J. Shiflet, Science **241**, 1640 (1988).
[7] A. P. Tsai, T. Kamiyama, Y. Kawamura, and A. Inoue, Acta Mater. **45**, 1477 (1997).
[8] A. Inoue, T. Zhang, and T. Masumoto, J. Non-Cryst. Solids **156–158**, 473 (1993).
[9] A. Inoue, T. Zhang, and T. Masumoto, Mater. Trans., JIM **36**, 391 (1995).
[10] A. Inoue, H. M. Kimura, and T. Masumoto, J. Mater. Sci. **16**, 1895 (1981); A. Inoue, T. Zhang, and T. Masumoto, Mater.

Trans., JIM **31**, 177 (1990).
[11] R. O. Suzuki, Y. Komatsu, K. E. Kobayashi, and P. H. Shingu, J. Mater. Sci. **18**, 1197 (1983).
[12] A. P. Tsai, A. Inoue, and T. Masumoto, J. Mater. Sci. Lett. **7**, 805 (1988).
[13] A. Inoue, K. Ohtera, A. P. Tsai, and T. Masumoto, Jpn. J. Appl. Phys. **27**, L479 (1988); G. J. Shiflet, Y. He, and S. J. Poon, J. Appl. Phys. **64**, 6863 (1988).
[14] Y. H. Kim, A. Inoue, and T. Masumoto, Mater. Trans., JIM **31**, 747 (1990); K. Suzuki, A. Makino, N. Kataoka, A. Inoue, and T. Masumoto, *ibid.* **32**, 93 (1991).
[15] H. Y. Hsieh, B. H. Toby, T. Egami, Y. He, S. J. Poon, and G. J. Shiflet, J. Mater. Res. **5**, 2807 (1990); H. Y. Hsieh, T. Egami, Y. He, S. J. Poon, and G. J. Shiflet, J. Non-Cryst. Solids **135**, 248 (1991).
[16] V. Sears, Neutron News **3**, 29 (1992).
[17] For reference see T. Egami and S. J. L. Billinge, in *Underneath the Bragg Peaks: Structural Analysis of Complex Materials*, Pergamon Materials Series, 2003, Vol. 7.
[18] B. E. Warren, *X-Ray Diffraction* (Dover, New York, 1969, 1990).
[19] B. H. Toby and T. Egami, Acta Crystallogr., Sect. A: Found. Crystallogr. **48**, 336 (1992).
[20] D. Louca, G. H. Kwei, B. Dabrowski, and Z. Bukowski, Phys. Rev. B **60**, 7558 (1999).
[21] S. R. Elliott, Phys. Rev. Lett. **67**, 711 (1991).
[22] D. Louca *et al.*, unpublished.
[23] V. Ponnambalam *et al.*, Appl. Phys. Lett. **83**, 1131 (2003).
[24] Y. Waseda, in *Structure of Non-Crystalline Materials* (McGraw-Hill, New York, 1980), p. 60.
[25] T. Egami and V. Vitek, in *Amorphous Materials: Modeling of Structure and Properties*, edited by V. Vitek (TMS-AIME, Warrendale, PA, 1983), p. 127.
[26] T. Egami and S. Aur, J. Non-Cryst. Solids **89**, 60 (1987).
[27] T. Egami, unpublished data.